JACS
JOURNAL OF THE AMERICAN CHEMICAL SOCIETY
Article
pubs.acs.org/JACS

"Texas-Sized" Molecular Boxes: Building Blocks for the Construction of Anion-Induced Supramolecular Species via Self-Assembly

Han-Yuan Gong,*[,†,‡] Brett M. Rambo,[†,§] Vincent M. Lynch,[†] Karin M. Keller,[†] and Jonathan L. Sessler*[,†,∥]

[†]Department of Chemistry and Biochemistry, The University of Texas at Austin, Welch Hall 2.204, 105 East 24th Street, Stop A5300, Austin, Texas 78712-1224, United States

[‡]College of Chemistry, Beijing Normal University, Beijing 100875, P. R. China

[§]Akermin Inc., 1005 North Warson Road, Suite 101, St. Louis, Missouri 63132, United States

[∥]Department of Chemistry, Yonsei University, Seoul 120-749, Korea

Supporting Information

ABSTRACT: It was previously established that the flexible tetraimidazolium macrocycle cyclo[2](2,6-bis(1*H*-imidazol-1-yl)pyridine)[2](1,4-dimethylenebenzene) ($\mathbf{1}^{4+}$) is capable of stabilizing higher-order supramolecular structures via both anion and cation recognition. Described herein is a set of structurally related imidazolium macrocycles ($\mathbf{2}^{4+}$–$\mathbf{4}^{4+}$) that contain modified central cores. The flexible nature of these new constructs is highlighted by the isolation of several independent crystalline forms for the same basic structure. Each of the individual receptors was found to bind the 2,6-naphthalenedicarboxylate dianion and to stabilize the formation of self-associated structures. The observed binding modes and resulting supramolecular organizational forms were found to differ dramatically depending on the nature of the bridging group present in the imidazolium macrocycle. This finding was established by solution studies involving, inter alia, one- and two-dimensional (^{1}H, ^{1}H–^{1}H COSY, DOSY, and NOESY) NMR spectroscopy as well as electrospray ionization mass spectrometry. The new systems in this report serve to expand the available "tool box" for the construction of complex self-assembled materials while providing insights into the determinants that regulate the formation of specific supramolecular structures from flexible receptors capable of adopting multiple stable conformations.

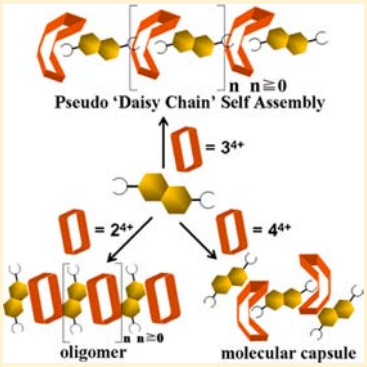

INTRODUCTION

Anions are ubiquitous in our environment and play important roles in both chemistry and biology. Not surprisingly, therefore, considerable effort over the last two decades has focused on the development of artificial receptors capable of interacting with various negatively charged species.[1−3] Among the many motifs used to effect anion recognition, C–H hydrogen-bonding donors have emerged as particularly attractive,[4−8] and considerable experimental and computational effort[9] has been devoted to understanding the underlying interactions. The imidazolium group is well-recognized for its ability to form strong $(C–H)^+–X^-$ hydrogen bonds[10] and for stabilizing charge–charge electrostatic interactions. This subunit has attracted considerable attention. For instance, Yoon and others have incorporated imidazolium subunits into a wide range of supramolecular receptors and studied their anion recognition properties in detail.[11−17] Early on, Alcalde et al.[18] reported heterophanes containing imidazolium moieties for anion recognition. Likewise, Xie and co-workers reported cyclophanes containing imidazolium as well as benzimidazolium groups.[19] In 2003, Sato et al. described the synthesis of a tetracationic heterophane that formed a 1:1 inclusion complex with halides and oxoanions in dimethyl sulfoxide-d_6 (DMSO-d_6).[20] Separately, imidazoliums and imidazolium-containing structures have received a great deal of attention for their ability to form carbenes upon deprotonation and thus stabilize various organometallic structures.[21−25]

Recently, our group reported the facile synthesis of a novel tetracationic imidazolium-based macrocycle, cyclo[2](2,6-bis(1*H*-imidazol-1-yl)pyridine)[2](1,4-dimethylenebenzene) ($\mathbf{1}^{4+}$), informally called the "Texas-sized" molecular box (Scheme 1).[26] Macrocycle $\mathbf{1}^{4+}$ was generated through a facile two-step synthetic route and isolated in a relatively high overall yield of 58%. This receptor differs from other known imidazolium macrocycles not only structurally but also in its inherent binding properties. The relatively large aromatic fragment [i.e., the portion containing the 2,6-bis(1*H*-imidazol-1-yl)pyridyl groups] allows for strong anion–π and π–π donor–acceptor interactions while maintaining a very high degree of flexibility. The innate flexibility incorporated into macrocycle $\mathbf{1}^{4+}$ is a salient feature that separates it from more rigid tetracationic receptors such as the well-studied "blue box" [cyclobis(paraquat-*p*-phenylene), $CBPQT^{4+}$] developed by Stoddart and co-workers.[27] Macrocycle $\mathbf{1}^{4+}$ has proven capable of forming supramolecular complexes with biscarboxylates with

Received: February 21, 2013
Published: March 21, 2013

 © 2013 American Chemical Society dx.doi.org/10.1021/ja401893w | *J. Am. Chem. Soc.* 2013, 135, 6330−6337

Scheme 1. Synthesis and Molecular Structures of the Tetraimidazolium Macrocycles Considered in This Study

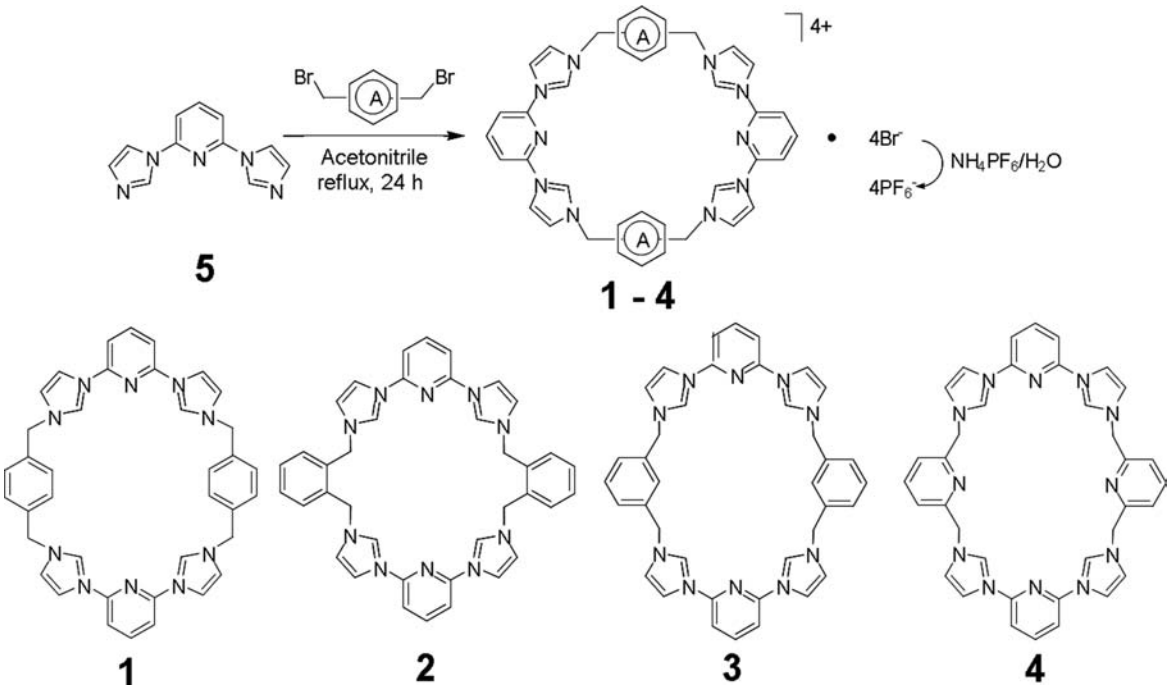

different sizes, shapes, and charges by altering its large central cavity into different shapes to accommodate a variety of anionic guests.[28,29] Furthermore, in some cases complexation with anionic biscarboxylates was found to result in the formation of threaded, or interpenetrated, pseudorotaxane complexes.[28−30] It was also demonstrated that the introduction of metal cations into the self-assembly process could be used to generate higher-order solid-state structures, including polyrotaxane chains,[28] metal−organic rotaxane frameworks (MORFs),[31,32] and rotaxane-containing supramolecular organic frameworks (RSOFs).[33]

The ability of $\mathbf{1}^{4+}$ to support the formation of a number of disparate supramolecular structures led us to consider whether structurally related macrocyclic systems might display similarly rich recognition chemistry. In an effort to address this question, we report three new tetracationic "Texas-sized" molecular boxes: $\mathbf{2}^{4+}$, $\mathbf{3}^{4+}$, and $\mathbf{4}^{4+}$. These new imidazolium-containing molecular receptors were prepared using the synthetic strategy employed to obtain $\mathbf{1}^{4+}$ (cf. Scheme 1) and were designed to allow direct comparisons to this earlier system. They also provide a complement to recent efforts from the Beer group to prepare large imidazolium-based macrocycles.[34] As detailed below and in analogy to $\mathbf{1}^{4+}$, the new macrocycles $\mathbf{2}^{4+}$, $\mathbf{3}^{4+}$, and $\mathbf{4}^{4+}$ proved to be quite flexible and were found to bind 2,6-naphthalenedicarboxylate dianion (**6**) in solution and in the solid state. However, the supramolecular complexes formed between macrocycles $\boldsymbol{n}^{4+}$ ($\boldsymbol{n}$ = **1**−**4**) and dianion **6** were found to display distinctly different stoichiometries. The resulting constructs are characterized by disparate binding modes. They also vary in their response to external stimuli (i.e., pH, temperature, and concentration). This versatility illustrates the "fine-tuning" that can be achieved by varying the macrocyclic structure within a congeneric series (in this case, by varying the nature of the bridging elements present in $\boldsymbol{n}^{4+}$). Studies with $\boldsymbol{n}^{4+}$ ($\boldsymbol{n}$ = **1**−**4**) also serve to underscore the important role that C−H hydrogen bonding can play in anion receptor design.

RESULTS AND DISCUSSION

Macrocycles $\mathbf{1}^{4+}$, $\mathbf{2}^{4+}$, $\mathbf{3}^{4+}$, and $\mathbf{4}^{4+}$ were prepared in good yields (59−71%; cf. Table 1) via an Ullmann-type coupling procedure involving the easily obtained fragment 2,6-bis(1*H*-imidazol-1-yl)pyridine (**5**)[26] and the commercially available precursors 1,4-, 1,2-, and 1,3-bis(bromomethyl)benzene and 2,6-bis-(bromomethyl)pyridine.

Table 1. Summary of the Percent Yields of Macrocycles Obtained from Different Substrates

entry	substrate	products	yield (%)
1	1,4-bis(bromomethyl)benzene	$\mathbf{1}^{4+}\cdot 4PF_6^-$	58
2	1,2-bis(bromomethyl)benzene	$\mathbf{2}^{4+}\cdot 4PF_6^-$	62
3	1,3-bis(bromomethyl)benzene	$\mathbf{3}^{4+}\cdot 4PF_6^-$	71
4	2,6-bis(bromomethyl)pyridine	$\mathbf{4}^{4+}\cdot 4PF_6^-$	65

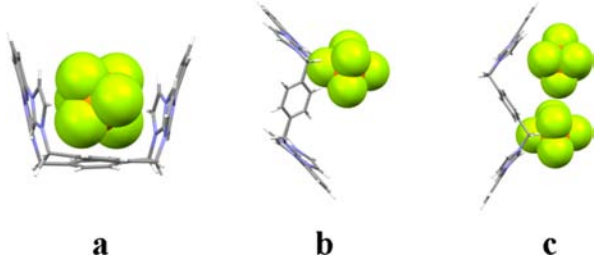

Figure 1. Three crystallographically independent single-crystal X-ray structures of $\mathbf{1}^{4+}\cdot 4PF_6^-$. Some or all of the counteranions and solvent molecules have been omitted for clarity. Included are (a) a side view showing the boatlike conformation of $\mathbf{1}^{4+}$ wherein one of four PF_6^- counteranions is held between the opposing aromatic faces, (b) a view of a second structure showing the partial chair conformation of $\mathbf{1}^{4+}$, and (c) a view of the third independent structure showing the more complete chair conformation of $\mathbf{1}^{4+}$.

Macrocycles $\mathbf{1}^{4+}$, $\mathbf{2}^{4+}$, $\mathbf{3}^{4+}$, and $\mathbf{4}^{4+}$ can be viewed as larger versions of $CBPQT^{4+}$. They are tetracationic macrocyclic

dx.doi.org/10.1021/ja401893w | J. Am. Chem. Soc. 2013, 135, 6330−6337

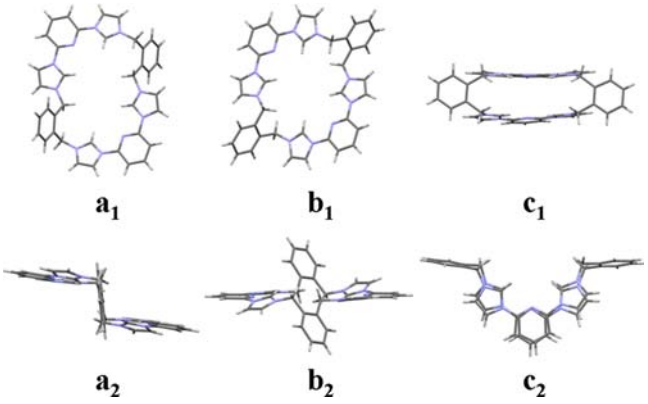

Figure 2. Crystallographically independent single-crystal X-ray structures of ($a_{1,2}$ and $b_{1,2}$) $\mathbf{2}^{4+}\cdot 4PF_6^-$ and ($c_{1,2}$) $\mathbf{2}^{4+}\cdot 2PF_6^-\cdot 2H_2PO_4^-\cdot 9.5H_2O$. All of the counteranions and solvent molecules have been omitted for clarity. (a_1) Top and (a_2) side views of $\mathbf{2}^{4+}\cdot 4PF_6^-$ showing the chairlike conformation of macrocycle $\mathbf{2}^{4+}$ present in this first structure. (b_1) Top and (b_2) side views showing the solid-state conformation that characterizes the second structure of $\mathbf{2}^{4+}\cdot 4PF_6^-$. ($c_1$) Top and ($c_2$) side views of the structure of $\mathbf{2}^{4+}\cdot 2PF_6^-\cdot 2H_2PO_4^-\cdot 9.5H_2O$ showing the "cliplike" conformation.

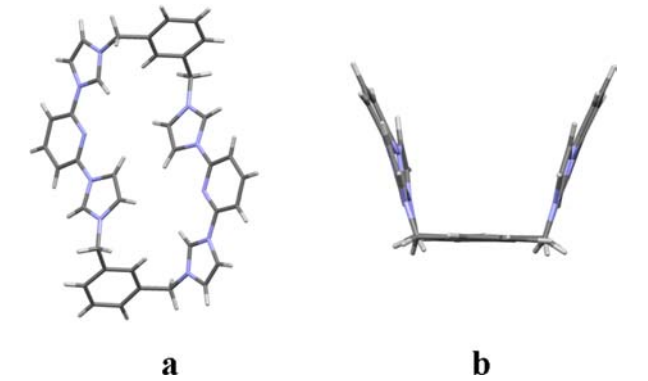

Figure 3. (a) Single-crystal X-ray structure of $\mathbf{3}^{4+}\cdot 4PF_6^-$. The view shown is designed to highlight the partial chair conformation observed in the solid state. (b) View of the boatlike conformation seen in the single-crystal structure of $\mathbf{3}^{4+}\cdot 4NO_3^-$. Counteranions and solvent molecules have been omitted for clarity.

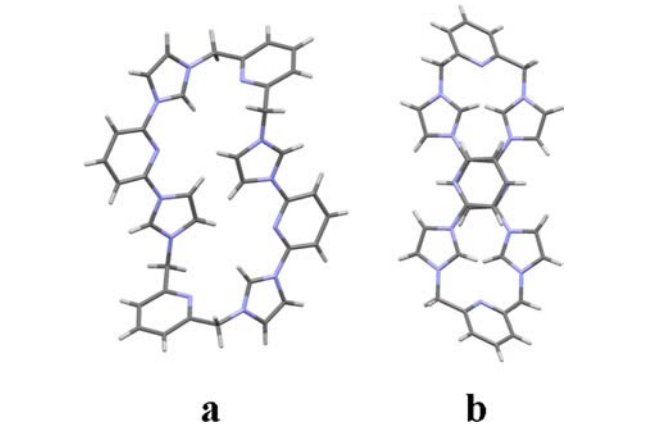

Figure 4. Two crystallographically independent single-crystal X-ray structures of $\mathbf{4}^{4+}\cdot PF_6^-$. All of the counteranions and solvent molecules have been omitted for clarity. The views shown are designed to highlight (a) the partial chair conformation seen in one of structures and (b) the helical conformation seen in the other.

structures that contain several aromatic π surfaces (i.e., benzene and pyridine moieties). However, in contrast to $CBPQT^{4+}$, macrocycles $\mathbf{1}^{4+}$, $\mathbf{2}^{4+}$, $\mathbf{3}^{4+}$, and $\mathbf{4}^{4+}$ are all characterized by an innate degree of flexibility. Nevertheless, as detailed below, each macrocycle within the series displays unique and distinct folding and substrate-binding modes.

Initial evidence for the flexible nature of macrocycles $\mathbf{1}^{4+}$, $\mathbf{2}^{4+}$, $\mathbf{3}^{4+}$, and $\mathbf{4}^{4+}$ came from ^{1}H NMR spectroscopic analyses. For each macrocycle, only one set of well-resolved signals was seen in the one-dimensional (1D) NMR spectrum recorded in DMSO-d_6 at room temperature, as would be expected for rapidly interconverting structures. Further analysis via two-dimensional (2D) nuclear Overhauser effect NMR spectroscopy (NOESY) revealed couplings that were consistent with the presence of more than one conformer in solution; this was true for all four macrocycles (cf. Supporting Information). Additional support for the conformational flexibility of macrocyclic structures $\boldsymbol{n}^{4+}$ ($\boldsymbol{n}$ = **1**–**4**) came from the isolation of single crystals of salts containing various counteranions, including PF_6^-, HPO_4^{2-} or $H_2PO_4^-$, and NO_3^-, and characterization of the resulting complexes via X-ray diffraction analysis.

The flexible nature of the original system (i.e., $\mathbf{1}^{4+}$) is highlighted by that fact that it has been characterized as its tetrakis(hexafluorophosphate) salt ($\mathbf{1}^{4+}\cdot 4PF_6^-$) in three crystallographically distinct polymorphic forms, as determined by single-crystal X-ray analysis. The first form is distinguished by the presence of a boatlike conformation for the macrocyclic core (cf. Figure 1a).[26] The second structure of this salt to be solved contains the same framework but exists in the form of a "partial chair" conformation (cf. Figure 1b).[26] In the context of the present work, the single-crystal structure of a third distinct form was solved; in this form, the macrocycle adopts a herringbone orientation, thus defining a more complete chair conformation (cf. Figure 1c). We also found that when other counteranions are used, two different conformations can be stabilized within a single-crystalline lattice, as evidenced by the structure of $\mathbf{1}^{4+}\cdot 2HPO_4^{2-}\cdot 9H_2O$ (cf. Supporting Information).

The flexible nature of $\mathbf{1}^{4+}$ and the isolation and structural characterization of three distinct crystalline forms of the tetra-PF_6^- salt provided an incentive to prepare analogues of this first-generation system. In particular, we were eager to determine how structural modifications of the macrocyclic core might affect the interactions with anions and the structures of the resulting salts. With this goal in mind, we started our investigation by creating analogues of $\mathbf{1}^{4+}$ based on the use of 1,2-bis(bromomethyl)benzene as a linking motif. In this case, single-crystal X-ray analyses allowed the characterization of two crystallographically distinct $\mathbf{2}^{4+}\cdot 4PF_6^-$ salts. A complete chair conformation of the cavity was present in the first structure (cf. Figure 2a). In contrast, the second structure revealed the same framework but in the context of a near-planar conformation in the solid state (Figure 2b).

A single crystal of the mixed anion salt $\mathbf{2}^{4+}\cdot 2PF_6^-\cdot 2H_2PO_4^-\cdot 9.5H_2O$ suitable for X-ray diffraction analysis was also obtained. In this case, a cliplike structure was observed in the solid state. Thus, taken in concert, these structures provide support for the notion that structural alterations in the original Texas-sized molecular box [e.g., changing the key precursor from 1,4- to 1,2-bis(bromomethyl)-benzene] can give rise to distinctly different structural conformations in the solid state.

Given the structural difference between the 1,2- and 1,4-bis(bromomethyl)benzene-derived isomers, we sought to

dx.doi.org/10.1021/ja401893w | J. Am. Chem. Soc. 2013, 135, 6330–6337

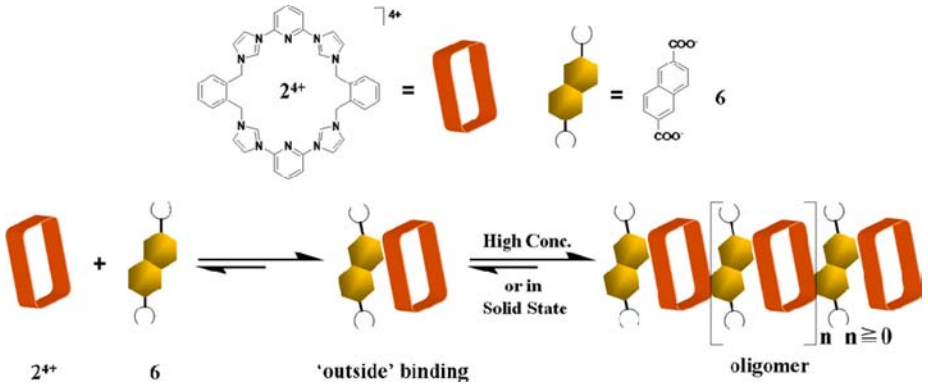

Figure 5. Schematic representation of the "outside" binding mode illustrating the interaction between host $\mathbf{2}^{4+}$ (as the PF_6^- salt) and guest **6** (as the $HTEA^+$ salt) as inferred from solution-phase ^1H NMR spectroscopic analyses in DMSO-d_6 and solid-state single-crystal X-ray diffraction analysis.

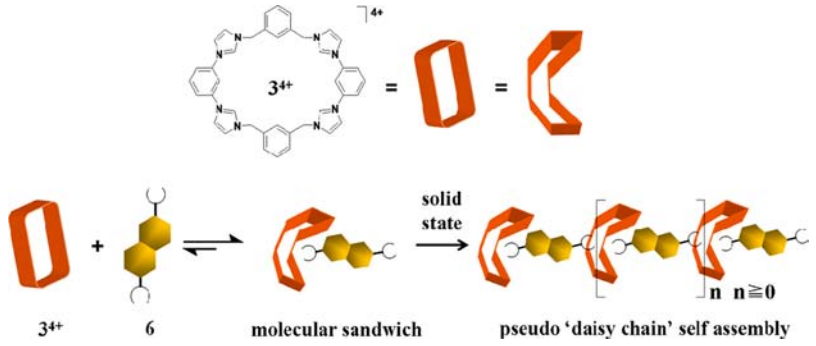

Figure 6. Schematic representation of the molecular sandwich complexes formed upon mixing of receptor $\mathbf{3}^{4+}$ (as the PF_6^- salt) and guest **6** (as the $HTEA^+$ salt) in a 1:1 ratio. The proposed structures, which feature an insert binding mode, were inferred from solution-phase ^1H NMR spectroscopic analyses in DMSO-d_6 and solid-state single-crystal X-ray diffraction analysis. It should be noted that more aggregated structures are stabilized in the solid state than are observed in solution.

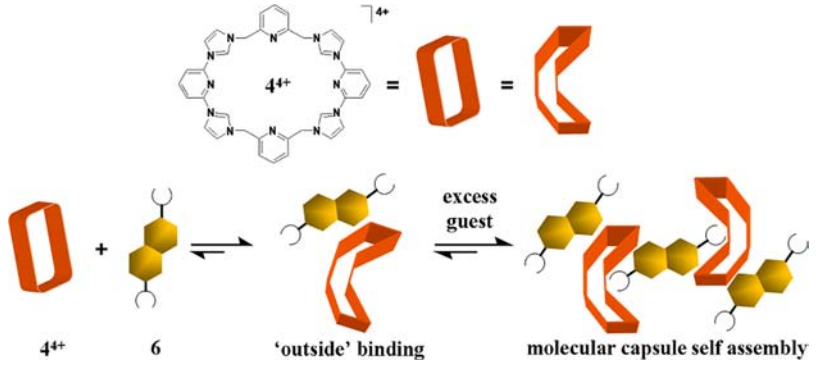

Figure 7. Schematic representation of the 1:1 "outside" binding mode proposed for the interaction of $\mathbf{4}^{4+}$ (as the PF_6^- salt) and guest **6** (as the $HTEA^+$ salt) and the proposed structure of the 2:3 H:G higher-order molecular aggregate $[(\mathbf{4}^{4+}\cdot\mathbf{6})\cdot\mathbf{6}\cdot(\mathbf{4}^{4+}\cdot\mathbf{6})]^{2+}$ seen at higher guest concentrations. These structures were inferred from solution-phase ^1H NMR spectroscopic analyses carried out in DMSO-d_6 and supported by solid-state single-crystal X-ray diffraction analysis.

analyze the corresponding 1,3-bis(bromomethyl)benzene-derived analogue $\mathbf{3}^{4+}$. In this case, only one structural conformation was observed for the hexafluorophosphate salt $\mathbf{3}^{4+}\cdot 4PF_6^-$ in the solid state, as inferred from repeated single-crystal X-ray structural analyses (Figure 3). This structure reveals that the tetrakis(imidazolium) macrocycle adopts a partial chair conformation in the solid state. In contrast, a single-crystal structural analysis of the corresponding nitrate salt $\mathbf{3}^{4+}\cdot 4NO_3^-$ (cf. Figure 2b) revealed the macrocycle in a boatlike conformation. Taken in concert, these results provide support for the conclusion that different conformations may be stabilized while likewise providing a hint that the $\mathbf{3}^{4+}$ system is perhaps less flexible than $\mathbf{1}^{4+}$ and $\mathbf{2}^{4+}$.

Macrocycle $\mathbf{4}^{4+}$ derived from 2,6-bis(bromomethyl)pyridine is structurally analogous to $\mathbf{3}^{4+}$. It was found to stabilize the formation of two crystallographically distinct structures for the hexafluorophosphate salt $\mathbf{4}^{4+}\cdot 4PF_6^-$ in the solid state. In the first of these structures, macrocycle $\mathbf{4}^{4+}$ adopts a partial chair conformation (Figure 4a); the structure thus bears resemblance to that observed in the case of $\mathbf{3}^{4+}\cdot 4PF_6^-$. A helical conformation was found in the second structure. This geometric arrangement is thought to be stabilized by strong $\pi-\pi$ donor–acceptor interactions involving the two bridged

dx.doi.org/10.1021/ja401893w | J. Am. Chem. Soc. 2013, 135, 6330–6337

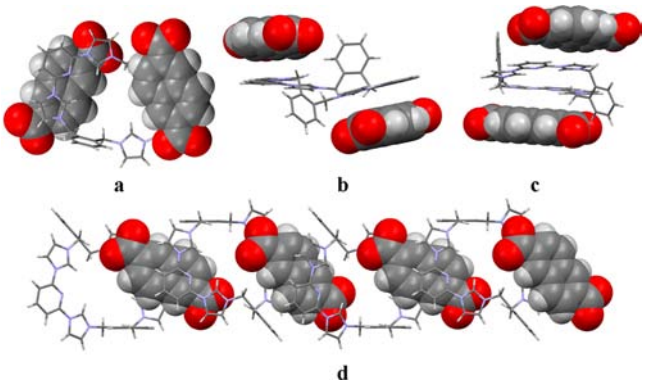

Figure 8. (a) Top, (b) side, and (c) front views of the single-crystal X-ray structure of the complex formed from $\mathbf{2}^{4+}$ and anionic guest **6** [i.e., $(\mathbf{2}^{4+}\cdot\mathbf{6}_2\cdot 17H_2O)$]. The complex exists as an extended structure with an overall 1:1 H:G ratio in the solid state; this self-assembled oligomeric material is stabilized by apparent $\pi-\pi$ interactions, as shown in the truncated view provided in (d). Some and/or all of the solvent molecules and counteranions have been omitted for clarity.

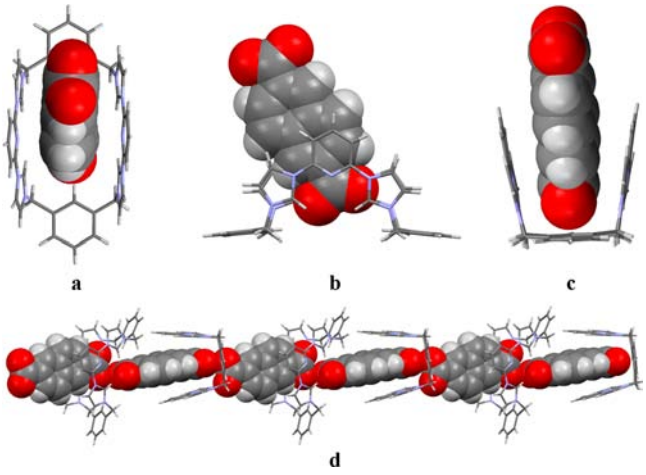

Figure 9. Views of the single-crystal X-ray structure of the molecular sandwich complex $(\mathbf{3}^{4+}\cdot\mathbf{6}_{1.5}\cdot OH^-\cdot H_2O)$ formed from $\mathbf{3}^{4+}$ and anionic guest **6**. Some and/or all of the solvent molecules and counteranions have been omitted for clarity. Top, side, and front views of the core complex are displayed in (a–c), respectively. Shown in (d) is a truncated view of the 1D molecular chain structure present in the solid state. The presence of individual "sandwichlike" subunits should be noted.

pyridine rings, as inferred from the short observed interatomic distances (i.e., less than 3.5 Å).

The structural information gained from single-crystal X-ray analysis of the salts of macrocycles $\boldsymbol{n}^{4+}$ ($\boldsymbol{n}$ = **1**–**4**) with PF_6^- and several other anions provides strong support for the conclusion that this new class of cyclic receptors is characterized by a high degree of inherent flexibility. Furthermore, while the anions were omitted from the views for the sake of clarity, the crystal structures presented above serve to confirm that these macrocycles are capable of binding anionic guests through a combination of C–H hydrogen bonds and anion–π donor–acceptor interactions (cf. Supporting Information). The hydrogen-bonding interactions are inferred from the short interatomic distances (less than 3.2 Å) between the imidazolium CH carbon atom and the F or O atoms present in the counteranion(s). Evidence for the proposed anion–π interactions comes from the relatively short interatomic distances (less than 3.8 Å) between the anionic guests and the neighboring aromatic ring(s) of the macrocyclic hosts.

The combination of a macrocyclic cavity that is inherently flexible with the ability to complex anionic guests through a variety of different binding modes led us to consider the possibility that the new tetracationic macrocycles $\mathbf{2}^{4+}$, $\mathbf{3}^{4+}$, and $\mathbf{4}^{4+}$ could be used as building blocks for the construction of higher-order supramolecular complexes, as had been noted previously in the case of $\mathbf{1}^{4+}$.[26,28−33]

To test this possibility, we investigated the ability of $\mathbf{2}^{4+}$, $\mathbf{3}^{4+}$, and $\mathbf{4}^{4+}$ to bind 2,6-napthalenedicarboxylate dianion (**6**) and subsequently form highly ordered supramolecular complexes. Solution and solid-state studies were conducted in tandem to probe the interactions between **6** and tetracations $\boldsymbol{n}^{4+}$ ($\boldsymbol{n}$ = **2**–**4**) [as the triethylammonium ($HTEA^+$) salt and the PF_6^- salts, respectively, unless otherwise indicated]. Initially, we investigated the complexation of **6** by $\mathbf{2}^{4+}$ using ^{1}H NMR spectroscopic methods. When a solution of $\mathbf{2}^{4+}$ in DMSO-d_6 was titrated with increasing concentrations of **6** in the same solvent, distinct changes in the original spectrum were observed. These changes were most notably in the chemical shifts of the imidazole C–H resonance and the aromatic peaks corresponding to **6**. Furthermore, NOESY studies revealed cross-peaks consistent with binding of **6** to the periphery of macrocycle $\mathbf{2}^{4+}$ via an "outside" binding mode (Figure 5).[28,29] Support for this latter postulate was later obtained by single-crystal X-ray analysis (vide infra). Job plot analysis also revealed a maximum value of 0.5 for the ratio [H]/([H] + [G]), a finding that is consistent with an overall 1:1 host: guest (H:G) binding stoichiometry in DMSO-d_6 solution. In addition, electrospray ionization mass spectrometry (ESI-MS) revealed a peak corresponding to $[\mathbf{2}^{4+}\cdot\mathbf{6} + H + Na]^{2+\bullet}$ (m/z 434.4) in the gas phase.

As a complement to the Job plot analyses, an isodesmic titration was performed. Here the changes in the chemical shift corresponding to the imidazole CH proton [H(1); cf. Supporting Information] were monitored as the solution concentration of guest **6** was increased while the concentration of host $\mathbf{2}^{4+}$ was held constant. Fitting to a 1:1 binding profile afforded an association constant (K_a) of $(2.3 \pm 0.1) \times 10^4$ M^{-1} for the formation of $[\mathbf{2}^{4+}\cdot\mathbf{6}]^{2+}$ in DMSO-d_6. This is a relatively high affinity given the postulated outside binding mode and is taken as evidence of the strong electrostatic attraction between what would be formally a tetracation ($\mathbf{2}^{4+}$) and a dianion (**6**) in the absence of residual ion-pairing effects involving the original counterions associated with $\mathbf{2}^{4+}$ and **6**.

As an extension to the above binding studies, a concentration-dependent ^{1}H NMR study involving $\mathbf{2}^{4+}$ and **6** was carried out. Here the change in the chemical shift corresponding to H(1) (cf. Supporting Information) was monitored as the overall solution concentration was increased while maintaining a constant 1:1 H:G ratio. As expected for an interacting system, spectral changes were seen as the overall solution concentration was increased. These changes were used to determine the association constants corresponding to the formation of the resulting dimeric, trimeric, and tetrameric structures: $([\mathbf{2}^{4+}\cdot\mathbf{6}]^{2+})_2$, $K_{a1} = (4.1 \pm 0.2) \times 10^2$ M^{-1}; $([\mathbf{2}^{4+}\cdot\mathbf{6}]^{2+})_3$, $K_{a2} = (2.8 \pm 0.2) \times 10^2$ M^{-1}; and $([\mathbf{2}^{4+}\cdot\mathbf{6}]^{2+})_4$, $K_{a3} = (1.5 \pm 0.1) \times 10^2$ M^{-1}, respectively (cf. Supporting Information). At very high concentrations, insoluble species, presumably polydisperse aggregates, were formed.

dx.doi.org/10.1021/ja401893w | J. Am. Chem. Soc. 2013, 135, 6330−6337

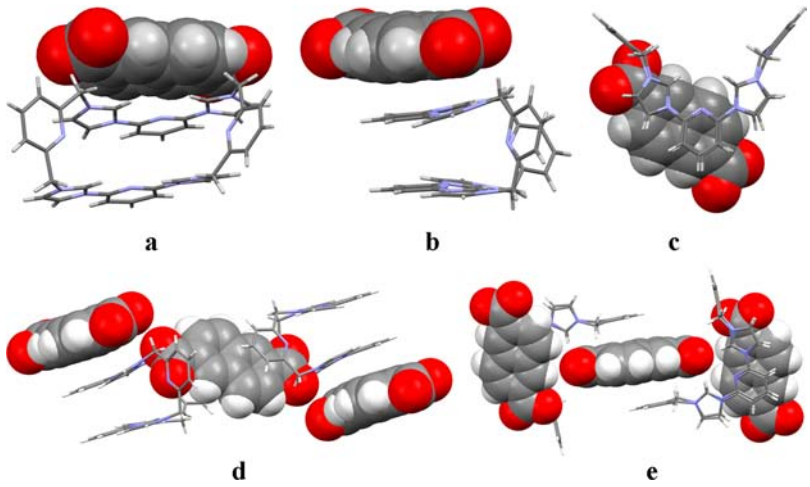

Figure 10. Views of the single-crystal X-ray structure of the complex ($4^{4+}\cdot 6_2\cdot 15H_2O$) formed from 4^{4+} and anionic guest **6**. Some and/or all of the solvent molecules and counteranions have been omitted for clarity. Top, side, and front views of the 1:1 complex $[4^{4+}\cdot 6]^{2+}$ highlighting the outside binding mode are displayed in (a–c), respectively. Views of the larger molecular capsule structure $[(4^{4+}\cdot 6)\cdot 6\cdot (4^{4+}\cdot 6)]^{2+}$ present in the lattice are shown in (d) and (e).

Similar solution studies involving 3^{4+} and **6** revealed a quite different binding pattern. Specifically, a Job plot analysis revealed a 1:1 binding stoichiometry in DMSO-d_6 solution (cf. Supporting Information). However, in contrast to what was seen for $[2^{4+}\cdot 6]^{2+}$, the formation of the $[3^{4+}\cdot 6]^{2+}$ complex was attributed to an "insert" binding mode (cf. Figure 6), with the excess positive charge balanced by PF_6^- anions. Initial support for the contention that the dianion **6** is "inserted" into 3^{4+} in $[3^{4+}\cdot 6]^{2+}$ came from single-crystal X-ray diffraction analysis, which revealed a molecular-sandwich-like structure in the solid state. A signal corresponding to the 1:1 complex was also seen in the gas phase via ESI-MS analysis ($[3^{4+}\cdot 6 - 2H]^{+\bullet}$, m/z 842.8).[35] In a separate study, NOESY analyses of the presumed complex cation $[3^{4+}\cdot 6]^{2+}$ were carried out at room temperature in DMSO-d_6. In the spectra, correlations between H(1) and H(6a–c), H(2) and H(6a–c), H(3) and H(6a), H(4) and H(6b,c), H(5) and H(6c), H(8) and H(6a–c), and H(9) and H(6a–c) were observed, which revealed cross-peaks consistent with the formation of an interpenetrated molecular complex as proposed (cf. Supporting Information for the relevant spectra).

From ^{1}H NMR-based isodesmic titrations, carried out in analogy to those involving 2^{4+} and **6** as described above, a K_a value of $(3.2 \pm 0.2) \times 10^4$ M^{-1} was derived for the formation of complex $[3^{4+}\cdot 6]^{2+}$ (cf. Figure 6 and Supporting Information). However, in marked contrast to what was observed in the case of 1:1 mixtures of 2^{4+} and **6**, no evidence for the formation of dimeric or trimeric species (either linear or sandwich-type) in DMSO-d_6 solution was seen in the case of $[3^{4+}\cdot 6]^{2+}$; this proved true even though pseudo-"daisy chain" self-assembled structures were found in the solid state (cf. Supporting Information).

The disparity in the binding behavior observed for macrocyclic hosts 2^{4+} and 3^{4+} in their interactions with **6** provided an incentive to study the interactions between macrocycle 4^{4+} and dianion **6**. In this case, the ^{1}H NMR-based titration in which **6** in DMSO-d_6 was added to a solution of 4^{4+} in the same solvent gave rise to changes in the spectrum consistent with the formation of a 2:3 complex (i.e., $[(4^{4+}\cdot 6)\cdot 6\cdot (4^{4+}\cdot 6)]^{2+}$). Binding constants $K_{a1} = (7.9 \pm 0.2) \times 10^3$ M^{-1} for the formation of an initial 1:1 complex and $K_{a2} = (7.3 \pm 0.2) \times 10^6$ M^{-2} for the formation of the subsequent 2:3 complex were derived from an isodesmic titration carried out as described above (cf. Supporting Information). Separately, NOESY analyses provided support for the inference that in this 1:1 complex, dianion **6** is located outside the macrocyclic cavity (cf. Supporting Information for the relevant spectra). The K_{a1} value corresponding to the formation of the 1:1 complex $[4^{4+}\cdot 6]^{2+}$ is significantly lower than that observed for the formation of $[3^{4+}\cdot 6]^{2+}$. This could reflect the relatively reduced ability of 4^{4+} to act as an external hydrogen-bond donor in comparison with 3^{4+}, presumably as the result of competing intramolecular imidazolium–pyridine CH–N hydrogen bonds. It could also reflect a conformation that is less suitable for the stabilization of π–π donor–acceptor interactions. Some support for these considerations came from solid-state single-crystal structural analyses, as discussed further below.

During the titration process, the signal of the protons on the bridging methylene-linked pyridine groups were found to shift to higher field. Concurrently, a very small shift in the signal corresponding to the protons on the pyridine rings directly linked to two flanking imidazolium groups was observed. This result leads us to suggest that the former subunits stabilized stronger π–π donor–acceptor interactions with the anionic guest. Specifically, on this basis, we postulate that macrocycle 4^{4+} interacts with **6** to form a 1:1 species, as shown in Figure 7. We also propose that higher-order aggregates of overall 2:3 H:G stoichiometry, such as $[(4^{4+}\cdot 6)\cdot 6\cdot (4^{4+}\cdot 6)]^{2+}$, are stabilized in the presence of excess guest **6** via a combination of further π–π donor–acceptor interactions involving dianion **6** and the bridging pyridine groups of receptor 4^{4+}. Evidence for the formation of such multicomponent species was obtained in the gas phase (e.g., a peak at m/z 955.1 ascribable to $[(4^{4+})_2 + (6)_3 + 2H]^{2+\bullet}$ was seen in the ESI-MS spectrum). An overall aggregated structure containing such 2:3 H:G subunits was also found in the solid state, as determined via single-crystal X-ray diffraction analysis (vide infra). As in the case of 3^{4+}, the absence of higher-order structures was inferred from concentration-dependent ^{1}H NMR spectroscopic studies (cf. Supporting Information).

As might be expected given the non-covalent nature of the complexes, the supramolecular structures formed from the

dx.doi.org/10.1021/ja401893w | J. Am. Chem. Soc. 2013, 135, 6330–6337

hosts and guest considered in this study (i.e., $([\mathbf{2}^{4+}\cdot\mathbf{6}]^{2+})_n$ ($n \geq 1$), $[\mathbf{3}^{4+}\cdot\mathbf{6}]^{2+}$, and $[\mathbf{4}^{4+}\cdot\mathbf{6}]^{2+}$) were found to be very sensitive to external stimuli (e.g., pH, temperature, and concentration). The effect of proton concentration was found to be substantial. Specifically, ^{1}H NMR spectroscopic studies involving dianion **6** and its fully protonated form $\mathbf{6}\cdot 2H^+$ in concert with the new receptors in this study revealed resonances for H(1) on $\boldsymbol{n}^{4+}$ ($\boldsymbol{n}$ = **2**–**4**) that shifted to lower field upon addition of triethylamine (TEA). A detailed analysis of the spectral changes that occurred as a function of added base led to the conclusion that stable complexes involving the dianionic species (i.e., **6**) were produced in the presence of TEA. On the other hand, the addition of deuterated trifluoroacetic acid (CF_3CO_2D) to solutions containing $[\boldsymbol{n}^{4+}\cdot\mathbf{6}]^{2+}$ ($\boldsymbol{n}$ = **2**–**4**) was found to cause decomposition of the complexes, with regeneration of fully protonated $\mathbf{6}\cdot 2H^+$ and release of the free receptor $\boldsymbol{n}^{4+}$ ($\boldsymbol{n}$ = **2**–**4**). This process of complex formation and proton-induced dissociation could be repeated, thus allowing the nature of the species present in solution to be controlled at will (cf. Supporting Information).

Further support for the responsive nature of the complexes formed between **6** and $\boldsymbol{n}^{4+}$ ($\boldsymbol{n}$ = **2**–**4**) came from variable-temperature ^{1}H NMR spectroscopic studies carried out in DMSO-d_6. These studies revealed losses in the signals corresponding to the complex in question, specifically in the H(1) peak associated with the imidazole C–H, which shifted toward the position ascribed to the nonassociated host as the temperature was increased (cf. Supporting Information). Such a finding is consistent with the formation of complexes stabilized by weak intermolecular hydrogen bonds and donor–acceptor interactions as opposed to more robust covalent or mechanical bonds.

Additional support for this conclusion came from concentration-dependent ^{1}H NMR spectroscopic studies carried out in DMSO-d_6. Specifically, it was found that the relative integrated intensities of peaks ascribable to 1:1 and higher-order complexes (e.g., $([\mathbf{2}^{4+}\cdot\mathbf{6}]^{2+})_n$ ($n \geq 1$), $[\mathbf{3}^{4+}\cdot\mathbf{6}]^{2+}$, or $[\mathbf{4}^{4+}\cdot\mathbf{6}]^{2+}$) increased relative to those ascribable to the uncomplexed macrocyclic host as the concentrations of **6** and $\boldsymbol{n}^{4+}$ ($\boldsymbol{n}$ = **2**–**4**) were increased while maintaining a 1:1 H:G ratio (cf. Supporting Information).

The studies described above provide evidence that hosts $\mathbf{2}^{4+}$, $\mathbf{3}^{4+}$, and $\mathbf{4}^{4+}$ are capable of stabilizing complex structures in the presence of dianion **6** in appropriately chosen organic media. To complement these solution-phase studies, single-crystal X-ray diffraction analyses were carried out. As detailed below, these studies provided evidence for the formation of supramolecular complexes and aggregates in the solid state as well as insights into the underlying binding modes.

The single-crystal X-ray structure of complex $[\mathbf{2}^{4+}\cdot\mathbf{6}]^{2+}$ (Figure 5) revealed that, as inferred from the solution-state NMR spectroscopic analyses discussed above, the dianionic guest species is located outside of macrocycle $\mathbf{2}^{4+}$. This stands in contrast to the pseudorotaxane binding mode observed in $[\mathbf{1}^{4+}\cdot\mathbf{6}]^{2+}$.[28,29] However, in the case of $[\mathbf{2}^{4+}\cdot\mathbf{6}]^{2+}$, the macrocycle adopts a slightly different structural conformation than it does in the case of the PF_6^- and mixed-anion salts discussed above (cf. Figure 2). In the case of complex $[\mathbf{2}^{4+}\cdot\mathbf{6}]^{2+}$, the macrocyclic core adopts a "twisted chair" conformation as opposed to the "complete chair", "near-planar", and "cliplike" conformations observed in the single crystal of its PF_6^- salt (cf. Supporting Information for further details). The twisted chair conformation seen in $[\mathbf{2}^{4+}\cdot\mathbf{6}]^{2+}$ results in a decreased cavity size and an orifice that is apparently unable to accommodate the threading of the dianionic guest **6**; as a result, "outside binding" of the dianion is observed. This interaction results in the formation of a 1D self-assembled oligomeric aggregate in the solid state that is stabilized via apparent intermolecular π–π interactions (Figure 8d). This structure is analogous to that inferred in solution at high concentration as discussed above (cf. Figures 5 and 8, as well as the Supporting Information).

The host containing the 1,3-dimethylphenyl bridges (i.e., $\mathbf{3}^{4+}$) has a cavity that is "wider" than that present in $\mathbf{2}^{4+}$ but "narrower" than that in the original host $\mathbf{1}^{4+}$, as determined from X-ray diffraction analysis of single crystals of $(\mathbf{3}^{4+}\cdot\mathbf{6}_{1.5}\cdot OH^-\cdot H_2O)$. In this case, the macrocycle adopts a "cliplike" conformation. Specifically, the bottom "half" of $\mathbf{3}^{4+}$ in this complex is characterized by a width of 5.0 Å, which is intermediate between the corresponding widths of 5.8 and 3.1 Å observed in the PF_6^- complexes of $\mathbf{1}^{4+}$ and $\mathbf{2}^{4+}$, respectively.

The aperture width of 7.1 Å for the macrocycle in complex $[\mathbf{3}^{4+}\cdot\mathbf{6}]^{2+}$ was found to be intermediate between those observed for the PF_6^- salts of $\mathbf{1}^{4+}$ and $\mathbf{2}^{4+}$ (9.4 and 3.9 Å, respectively; vide supra). In the solid state, macrocycle $\mathbf{3}^{4+}$ complexes guest **6** in a cliplike fashion. The dianion is held between two 2,6-bis(1*H*-imidazol-1-yl)pyridine fragments via strong $\pi\cdots\pi$ donor–acceptor interactions, as inferred from the short interatomic distance observed (less than 3.5 Å). This 1:1 binding results in the formation of a molecular sandwich structure that corresponds well with what was inferred on the basis of the solution-phase studies (vide supra). Finally, it was observed that one molecular sandwich could be inserted into the cavity of a neighboring complex to form a 1D supramolecular polymeric chain in the solid state (cf. Figure 9 and the Supporting Information).

As highlighted by the solution studies described above, receptor $\mathbf{4}^{4+}$ differs from $\mathbf{3}^{4+}$ in terms of its interactions with **6**. In $\mathbf{3}^{4+}$, the CH subunit present on the bridging benzene rings points to the inside of the cavity. However, such a putative hydrogen-bond donor is not present in the case of $\mathbf{4}^{4+}$ since the CH group in question has been replaced by a nitrogen atom. This CH-for-N replacement presumably underlies the stabilization of structurally distinct binding modes in the solid state. In the case of $\mathbf{4}^{4+}$, interactions with **6** result in binding of the guest to the outside of the macrocycle, and the addition of excess guest molecule was found to link two 1:1 complex units; the net result is a molecular capsule structure stabilized by π–π donor–acceptor interactions between certain regions of the guest-plane π surfaces and the bridged pyridine rings on different molecules of $\mathbf{4}^{4+}$ (cf. Figure 10 and the Supporting Information).

The solid-state studies described above detail a wide variety of binding modes for macrocycles $\boldsymbol{n}^{4+}$ (n = **2**–**4**) and dianion **6**. The conformers observed in the absence of added guest **6** were found to be highly dependent on the choice of the bridging group. These same structural alterations were observed to result in significantly different solid-state complexes in the presence of **6**. The nature of the binding modes seen in these complexes ranged from outside binding in $[\mathbf{2}^{4+}\cdot\mathbf{6}]^{2+}$ to molecular clips that self-assemble into linear polymers in $[\mathbf{3}^{4+}\cdot\mathbf{6}]^{2+}$. This diversity was observed using a single dianionic guest (i.e., **6**), a finding that underscores the fact that the observed structural changes arise from connectivity modifications within the tetraimidazolium receptors per se, as opposed to some external effect.

dx.doi.org/10.1021/ja401893w | J. Am. Chem. Soc. 2013, 135, 6330–6337

CONCLUSION

We have detailed the synthesis, structure, and initial substrate recognition properties of the new family of congeneric macrocyclic tetraimidazolium receptors $\boldsymbol{n}^{4+}$ (n = **1**–**4**). The synthesis of these "Texas-sized" boxes proved to be facile, efficient, and readily generalizable, at least within the context of this matched set of tetracationic macrocycles. In the case of the new receptors $\mathbf{2}^{4+}$, $\mathbf{3}^{4+}$, and $\mathbf{4}^{4+}$, various combinations of C–H hydrogen-bonding, anion–π, and π–π donor–acceptor interactions serve to stabilize the binding of the tested guest, 2,6-naphthalenedicarboxylate dianion (**6**). The nature of the resulting complexes was inferred on the basis of 1D and 2D ^{1}H NMR spectroscopic studies carried out in DMSO-d_6, ESI-MS studies, and X-ray diffraction analyses. The diversity of structures obtained is considered to reflect the fact that receptors $\mathbf{2}^{4+}$, $\mathbf{3}^{4+}$, and $\mathbf{4}^{4+}$ are inherently flexible, with the specific nature of the species formed being highly dependent on the bridging group (i.e., on the choice of receptor). The present findings lead us to propose that receptors $\boldsymbol{n}^{4+}$ (n = **1**–**4**) and their congeners may have a role to play in the construction of higher-order self-assembled systems with rationally designed organizational features.

ASSOCIATED CONTENT

Supporting Information

Synthetic experimental section, details of NMR spectroscopic and single-crystal X-ray diffraction analyses, and crystallographic data in CIF format. This material is available free of charge via the Internet at http://pubs.acs.org.

AUTHOR INFORMATION

Corresponding Author

hyg2070@iccas.ac.cn; sessler@cm.utexas.edu

Notes

The authors declare no competing financial interest.

ACKNOWLEDGMENTS

The authors are grateful to the National Science Foundation (Grant CHE 1057904 to J.L.S. and Grant 0741973 for the X-ray diffractometer) and the Robert A. Welch Foundation (Grant F-1018 to J.L.S.) for financial support. Thanks also go to S. Sorey and J.-F. Xiang for their assistance with the NMR spectroscopic analyses. J.L.S. also thanks the World Class University (WCU) Program of Korea (*R*32-2008-000-10217-0). H.-Y.G. is also grateful to the National Natural Science Foundation of China (21202199), The Young One-Thousand-Talents Scheme, and Beijing Normal University for financial support.

REFERENCES

(1) Gale, P. A. *Chem. Commun.* **2011**, *47*, 82–86.

(2) Sessler, J. L.; Gale, P. A.; Cho, W.-S. *Anion Receptor Chemistry*; Monographs in Supramolecular Chemistry, Stoddart, J. F., Series Ed.; Royal Society of Chemistry: Cambridge, U.K., 2006.

(3) Wenzel, M.; Hiscock, J. R.; Gale, P. A. *Chem. Soc. Rev.* **2012**, *41*, 480–520.

(4) Hua, Y.; Ramabhadran, R. O.; Uduehi, E. O.; Karty, J. A.; Raghavachari, K.; Flood, A. H. *Chem.—Eur. J.* **2011**, *17*, 312–321.

(5) Hua, Y.; Flood, A. H. *Chem. Soc. Rev.* **2010**, *39*, 1262–1271.

(6) Vega, I. E. D.; Gale, P. A.; Light, M. E.; Loeb, S. J. *Chem. Commun.* **2005**, 4913–4915.

(7) Sessler, J. L.; Cai, J.; Gong, H.-Y.; Yang, X.; Arambula, J. F.; Hay, B. P. *J. Am. Chem. Soc.* **2010**, *132*, 14058–14060.

(8) Ilioudis, C. A.; Tocher, D. A.; Steed, J. W. *J. Am. Chem. Soc.* **2004**, *126*, 12395–12402.

(9) Quinonero, C.; Deya, P. M.; Carranza, P. M.; Rodriguez, A. M.; Jalon, F. A.; Manzano, B. R. *Dalton Trans.* **2010**, *39*, 794–806.

(10) Ihm, H.; Yun, S.; Kim, H. G.; Kim, J. K.; Kim, K. S. *Org. Lett.* **2002**, *4*, 2897–2900.

(11) Alcalde, E.; Dinares, I.; Mesquida, N. *Top. Heterocycl. Chem.* **2010**, *24*, 267–300.

(12) Willans, C. E.; Anderson, K. M.; Potts, L. C.; Steed, J. W. *Org. Biomol. Chem.* **2009**, *7*, 1500–1516.

(13) Khatri, V. K.; Chahar, M.; Pavani, K.; Pandrey, P. S. *J. Org. Chem.* **2007**, *72*, 10224–10226.

(14) Xu, Z.; Singh, N. J.; Sook, K.; Spring, D. R.; Kim, K. S.; Yoon, J. *Chem.—Eur. J.* **2011**, *17*, 1163–1170.

(15) Xu, Z.; Kim, S. K.; Yoon, J. *Chem. Soc. Rev.* **2010**, *39*, 1457–1466.

(16) Yoon, J.; Kim, S. K.; Singh, N. J.; Kim, K. S. *Chem. Soc. Rev.* **2006**, *35*, 355–360.

(17) Thomas, J.-L.; Howarth, J.; Hanlon, K.; McGuirk, D. *Tetrahedron Lett.* **2000**, *41*, 413–416.

(18) Alcalde, E.; Alvarez-Rúa, C.; García-Granda, S.; García-Rodriguez, E.; Mesquida, N.; Pérez-García, L. *Chem. Commun.* **1999**, 295–296.

(19) Yuan, Y.; Gao, G.; Jiang, Z.-L.; You, J.-S.; Yuan, D.-Q.; Xie, R.-G. *Tetrahedron* **2002**, *58*, 8993–8999.

(20) Sato, K.; Arai, S.; Yamagishi, T. *Heterocycles* **2003**, *60*, 779–784.

(21) Arduengo, A. J.; Harlow, R. L.; Kline, M. *J. Am. Chem. Soc.* **1991**, *113*, 361–363.

(22) Radloff, C.; Gong, H.-Y.; Brinke, C. S. T.; Pape, T.; Lynch, V. M.; Sessler, J. L.; Hahn, F. E. *Chem.—Eur. J.* **2010**, *16*, 13077–13081.

(23) Potayos, M.; Mata, J. A.; Peris, E. *Chem. Rev.* **2009**, *109*, 3677–3707.

(24) Hahn, F. E.; Jahnke, M. C. *Angew. Chem.* **2008**, *120*, 3166–3216.

(25) Bourissou, D.; Guerret, O.; Gabbaï, F. P.; Bertrand, G. *Chem. Rev.* **2000**, *100*, 39–91.

(26) Gong, H.-Y. ; Rambo, B. M.; Karnas, E.; Lynch, V. M.; Sessler, J. L. *Nat. Chem.* **2010**, *2*, 406–409.

(27) Odell, B.; Reddington, M. V.; Slawin, A. M. Z.; Spencer, N.; Stoddart, J. F.; Williams, D. J. *Angew. Chem., Int. Ed. Engl.* **1988**, *27*, 1547–1550.

(28) Rambo, B. M.; Gong, H.-Y.; Oh, M.; Sessler, J. L. *Acc. Chem. Res.* **2012**, *45*, 1390–1401.

(29) Gong, H.-Y. ; Rambo, B. M.; Karnas, E. K.; Lynch, V. M.; Keller, K. M.; Sessler, J. L. *J. Am. Chem. Soc.* **2011**, *133*, 1526–1533.

(30) Gong, H.-Y. ; Rambo, B. M.; Lynch, V. M.; Keller, K. M.; Sessler, J. L. *Chem.—Eur. J.* **2012**, *18*, 7803–7809.

(31) Gong, H.-Y.; Rambo, B. M.; Cho, W.; Lynch, V. M.; Oh, M.; Sessler, J. L. *Chem. Commun.* **2011**, *47*, 5973–5975.

(32) Gong, H.-Y.; Rambo, B. M.; Nelson, C. A.; Lynch, V. M.; Zhu, X.; Sessler, J. L. *Chem. Commun.* **2012**, *48*, 10186–10188.

(33) Gong, H.-Y.; Rambo, B. M.; Nelson, C. A.; Cho, W.; Lynch, V. M.; Zhu, X.; Oh, M.; Sessler, J. L. *Dalton Trans.* **2012**, *41*, 1134–1137.

(34) Serpell, C. J.; Cookson, J.; Thompson, A. L.; Beer, P. D. *Chem. Sci.* **2011**, *2*, 494–500.

(35) The supramolecular species have different apparent charges in the gas phase than in solution. This apparent disparity is thought to reflect the formation of various cation radicals under the conditions of mass spectrometric analysis as the result of proton-transfer processes.